

## Coherent and self-amplified infrared synchrotron radiation emitted by a 50-MeV electron beam

J. M. Ortega, R. Prazeres, F. Glotin, and D. A. Jaroszynski\*  
*LURE, Bâtiment 209d, Université de Paris-Sud, 91405 Orsay Cedex, France*  
 (Received 23 July 1997)

We have observed and analyzed the coherent spontaneous emission (CSE) and the self-amplified spontaneous emission (SASE) emitted, in the near infrared spectral range, by short pulses of relativistic electrons passing through an undulator. The CSE is surprisingly large at wavelengths much shorter than the electron pulse length. The SASE spectral line exhibits an unexpected growth at the start-up of the process. Both phenomena are fluctuating and can be distinguished only by careful spectral measurements.

[S1063-651X(97)10512-8]

PACS number(s): 41.60.Cr, 41.50.+h

### I. INTRODUCTION

A relativistic electron beam crossing a transverse field, usually a periodic magnetic “undulator” produces synchrotron radiation (called “spontaneous emission” or “radiation noise”). This radiation is very interesting in itself and is widely used as a source in synchrotron radiation centers. This radiation can be extraordinarily more intense when all electrons radiate in phase: this happens when the electrons are longitudinally bunched in substructures of length comparable to the radiation wavelength. This is usually called “coherent spontaneous emission,” when these substructures exist before the electrons are entering the field and “stimulated emission” or “free-electron laser” (FEL) when a beam longitudinal modulation is produced by interaction with the optical and magnetic fields. The FEL is widely used as a source of such intense radiation [1,2]. In a FEL, an undulator is placed in an optical cavity which stores the stimulated spontaneous emission. This stimulated emission is subsequently amplified at each pass through the electron beam, up to the saturation level. The wavelength is tunable over a large range, by sweeping the magnetic field of the undulator and the electron beam energy. There are FELs operating in various wavelength regions from millimeter waves to ultraviolet [1,2]. In principle, the FEL will operate in the x-ray spectral range. However, the state of the art of optical cavity mirrors and electron beams has not been sufficient to produce FEL oscillation at wavelengths shorter than 240 nm [3]. Other related techniques, noticeably the VUV harmonic generation in an undulator [4] and x-ray generation by FEL intracavity Compton backscattering [5] have been demonstrated, but are producing small power.

Another solution proposed [6] to reach the x-ray range is to operate with a very high gain in single pass configuration, thus avoiding mirrors: the spontaneous emission is amplified in a very long undulator (20–40 m), and reaches saturation in one pass. This so-called “self-amplified spontaneous emission” (SASE) requires a very high quality electron beam (high peak current, low energy spread, small emittance). Its

energy has to be quite high (several GeV) if one wants to reach the x-ray range, making the device extremely expensive and cumbersome. The SASE has so far only been observed in cm waves [7] and in the millimeter [8] spectral ranges. Indeed, the electron beam requirements needed for SASE are more and more demanding as the wavelength decreases. Thus, study of SASE in the midinfrared region is an important step in understanding the process and in extrapolating to the possible development of SASE sources in x-rays. Recently, we have been able to produce below saturation SASE in the spectral region of 5–10  $\mu\text{m}$  [9]. At this level of SASE, it is very difficult, however, to distinguish between the coherent spontaneous emission, due to the initial electron temporal distribution, and the SASE, which is caused by a self-induced modulation of this distribution. In the present paper, we analyze in detail the experimental behavior of these two phenomena.

Let us examine the different aspects of the radiation which may occur in such a radiating device, and which are the spontaneous emission, coherent spontaneous emission, FEL gain, and SASE.

(i) The spontaneous emission (SE) is the radiation produced by a single electron, traveling along an undulator of  $N$  magnetic periods. It is peaking at the so-called resonance wavelength:

$$\lambda_R = \lambda_u (1 + K^2/2) / 2\gamma^2,$$

where  $\lambda_u$  and  $K$  are, respectively, the period and the dimensionless “deflection parameter” of the undulator [9], and  $\gamma mc^2$  is the electron beam energy. The single electron radiation is a wave train of  $N$  periods, corresponding to a length of  $N\lambda_R$ . The spectral linewidth of the radiation is

$$\Delta\omega/\omega \cong 0.9/N.$$

Considering a bunch of  $N_e$  electrons, assuming they are randomly distributed in the bunch, the electrons are incoherent sources. The resulting amplitude of the emitted radiation has an averaged absolute value of  $(N_e)^{1/2}$  times the one-electron amplitude and the total intensity is simply  $N_e$  times the one-electron intensity. Therefore, the incoherent emission of an electron bunch is just  $N_e$  times the one-electron SE and the

\*Permanent address: Department of Physics and Applied Physics, University of Strathclyde, John Anderson Building, 107 Rottenrow, Glasgow G4 0NG, UK.

energy produced scales as  $N(N_e)$  [on-axis and in a relative bandpass  $< 1/N$ , this energy is proportional instead to  $N^2(N_e)$ , due to the undulator interference effect].

(ii) The coherent spontaneous emission (CSE) is observed if the dimension of the electron bunch is smaller than the emitted wavelength. In this case, the individual sources (electrons) are in phase and the amplitudes add linearly. The total emitted energy scales as  $N(N_e)^2$ , i.e., linearly with the undulator length, and quadratically with the electron current.  $N_e$  being usually large, the ratio of CSE over SE can be very large, of the order of  $10^8$  to  $10^{10}$ . In most FELs, including CLIO, the electron bunch length is larger than the emitted wavelength, and the CSE should be negligible. Nevertheless, a partial coherence still occurs if the electron bunch longitudinal density exhibits structures like sharp edges, or more generally, strong components at high frequency in its Fourier spectrum. In this case, a CSE component of intensity  $I_{\text{coh}}(\omega)$  adds to the SE intensity  $I_{\text{SE}}(\omega) = I_0(\omega)N_e$ , where  $I_0$  is the intensity emitted by one electron. This CSE component is described by the diffraction theory which yields a coherent intensity:

$$I_{\text{coh}}(\omega) = I_0(\omega)N_e^2 f^2(\omega),$$

where  $f(\omega)$  is the Fourier transform of the longitudinal electron density.

The total intensity is

$$I_T(\omega) = I_{\text{coh}} + I_{\text{SE}} \approx N(i + f^2 i^2),$$

where  $i$  is the electron beam average current.  $f$  is also a function of  $i$ , when the electron longitudinal shape varies with the average current.

Both SE and the CSE are ‘‘spontaneous emission’’ and have the same spectral distribution, equal to the one electron distribution if the function  $f(\omega)$  is ‘‘smooth.’’

(iii) Another method of increasing the emission of light is through the FEL gain process, induced by the interaction between the electron bunch and an optical wave, which creates a periodical modulation (microbunching) on the electron beam distribution, and produces a strong Fourier component at the resonant wavelength and possibly its harmonics: in this case  $f(\omega)$  becomes a sharply peaked function. This component adds to the initial optical wave and constitutes the ‘‘gain’’: with an adequate optical cavity, it produces the FEL oscillation [2]. The initial wave is then the stored spontaneous emission. When the spontaneous emission which is produced along the undulator is noticeably amplified in a single pass so as to enter an exponential growth regime, it is called self-amplified spontaneous emission (SASE). The analysis of this process has been carried out by several authors [6]. The power of SASE grows exponentially along the undulator axis  $z$ , with

$$P_{\text{SASE}} \propto \exp(z/L_g),$$

where

$$L_g = \lambda_u / (4\pi\rho\nu^3).$$

$L_g$  is the ‘‘gain length,’’ which characterizes the exponential growth of SASE and depends on a dimensionless ‘‘Pierce parameter,’’  $\rho$ , which is proportional to  $(\hat{i}/\sigma_e \gamma^3)$ .  $\hat{i}$

is the peak electron current,  $\sigma_e$  its transverse size, and  $\gamma mc^2$  its energy. When  $\rho$  is small, it becomes practically impossible to reach saturation. In practice, SASE requires higher intensities and smaller emittance (transverse size) as the energy increases, i.e., as the desired wavelength is smaller. The saturation occurs for  $\rho N \cong 1$ . At start-up ( $\rho N \ll 1$ ), the radiation is the spontaneous emission of an incoherent electron beam, the spectral width being  $\sim 1/N$ . In the exponential growth regime, one expects a reduction of the spectral line-width to  $\Delta\omega/\omega \cong (\rho N)^{1/2}/N$ .

At saturation, of either SASE or the FEL oscillator, the amplification of SE is also of the order of  $N_e$ , i.e., in the range of  $10^8 - 10^{10}$ .

The SE is intrinsically noisy. This noise is classical and adds to the quantum fluctuations. However, the amplitude of the classical fluctuations scales as  $1/(N_t)^{1/2}$ , where  $N_t$  is the number of electrons emitting in the observed solid angle and bandpass. Therefore, the SE is not fluctuating in most practical conditions. The CSE is, supposedly, classically not fluctuating, since all the electrons radiate in phase. However, at wavelengths shorter than the electron bunch length, the CSE is due to the details in the bunch longitudinal distribution and amplifies strongly any pulse to pulse variation. The SASE has been calculated to be intrinsically fluctuating below saturation [6]: The electron bunch distribution fluctuations (acting mainly on the peak current) can also cause large variations in the SASE exponential regime. The FEL oscillator reaching saturation is usually stable, although quite sensitive to the electron beam fluctuations [1,2,10].

## II. THE CLIO INFRARED FEL FACILITY

We present here the successful production and observation of CSE and SASE in the midinfrared region at  $\lambda \cong 5 \mu\text{m}$  and  $10 \mu\text{m}$ . These observations have been carried out with the ‘‘CLIO’’ FEL. CLIO is an infrared free-electron laser and a user facility since 1993 [10]. CLIO is based on a pulsed linear accelerator. (See Figs. 1 and 2.) Its characteristics are listed in Table I. CLIO is offering more than 2000 hours per year of beam time to users working mostly in the fields of surface and solid state physics, electrochemical interfaces, molecular dynamics, near-field microscopy, and medicine. Although devoted to users, CLIO is using some of the beam time to study FEL basic processes and improvements [4,5,9–12]. For example, the two-color FEL is an original property of CLIO [12], which enhances its capabilities in time resolved pump-probe experiments.

The accelerator delivers 12  $\mu\text{s}$  long trains of short pulses. This pulse length has been measured with a collimator placed in an energy dispersive section of the magnetic bend: the beam is dephased in the accelerating section so as to transform its time dependence into an energy dependence. The resolution of the method can be very good in principle. In our case it is limited by the fact that some bunch evolution may still occur in the long accelerating section and we estimated it to 1 ps (300  $\mu\text{m}$ ), well above the wavelengths of interest (5–10  $\mu\text{m}$ ). However, the pulse is very asymmetric [11] so that it may have Fourier components at short wavelengths.

The same collimator has been used to vary the beam current, in an effort to measure the current dependence of SASE

TABLE I. CLIO FEL main parameters.

Accelerator	
type	linear, radiofrequency, 3 GHz
gun	thermoionic, 1 ns pulse
prebuncher	500 MHz reentrant cavity
buncher	3 GHz, 5 MeV, SW
accelerator	3 GHz, 50 MeV, TW
maximum energy	50 MeV
minimum energy	20 MeV
peak current	100 A
magnetic bend	doubly achromatic
90% emittance	nearly isochronous ( $< 1$ ps/%)
energy spread (FWHM)	150 $\pi$ mm mrad (normalized)
	1%
Time structure	
macropulse length	11 $\mu$ s
repetition rate	1–50 Hz
micropulse length	8 ps (measured)
micropulse separation	4–32 ns
FEL	
undulator period	50.4 mm
number of periods: $N$	19 (for each undulator section)
measured gain per pass (laser rise time at start-up)	up to 500%
Pierce parameter: $\rho$	$1.9 \times 10^{-3}$
Laser range	3–53 $\mu$ m

and CSE. However, moving one slit across the beam selects parts of the beam having different energy distribution, which makes it more difficult to interpret the data. In fact, in an accelerator, it is difficult to find a way to vary the peak current while maintaining constant bunch shape and energy distribution.

The thermoionic gun makes the machine very reliable and

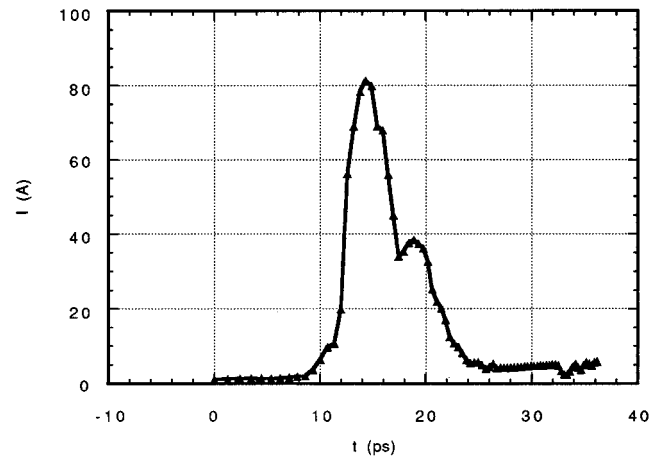


FIG. 2. Measured shape of the electron pulse.

stable. However, there are small instabilities in the bunch shape which produce large fluctuations on the observed CSE as well as on SASE. Also, the tuning of the machine is much more critical for CSE and SASE than for the FEL itself, the quadrupoles acting on the achromatism and the isochronism of the bend being particularly sensitive.

The CLIO spectral range spans 3–50  $\mu$ m at electron energies ranging from 50 to 20 MeV (Fig. 3). The present experiment has been performed at 50 MeV because, on one hand, we always observed a better FEL at this energy and, on the other hand, in order to avoid too much CSE, since the observed SASE is far from saturation. Optical gain of up to 4 has been measured on the FEL oscillator, which has led us to think that SASE should be readily observable on CLIO. (See Fig. 4.)

The undulator of CLIO has 38 magnetic periods, divided in two half-undulator sections of  $N=19$  periods, for which each gap is independently adjustable. This feature is made to run the FEL in a two-color mode [12], but it also should allow discrimination between SASE and CSE effects, since

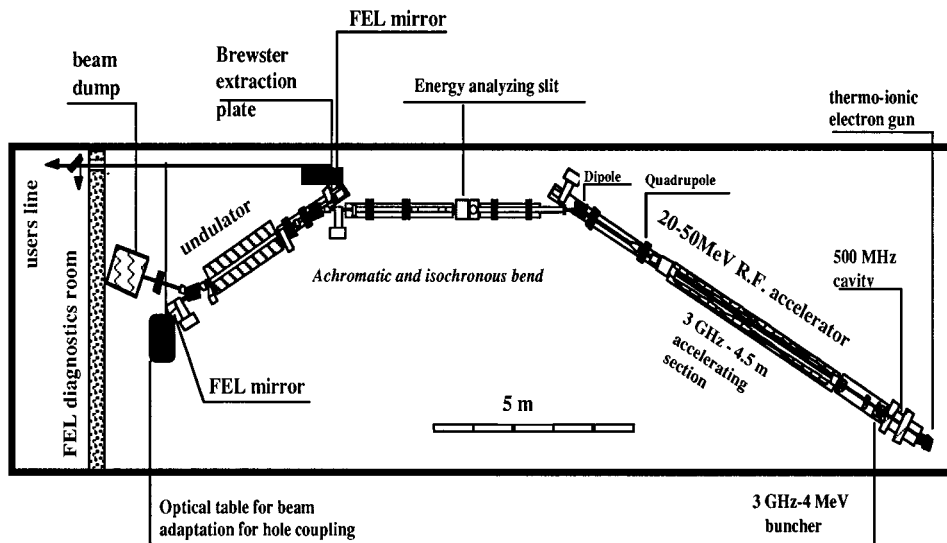


FIG. 1. CLIO layout.

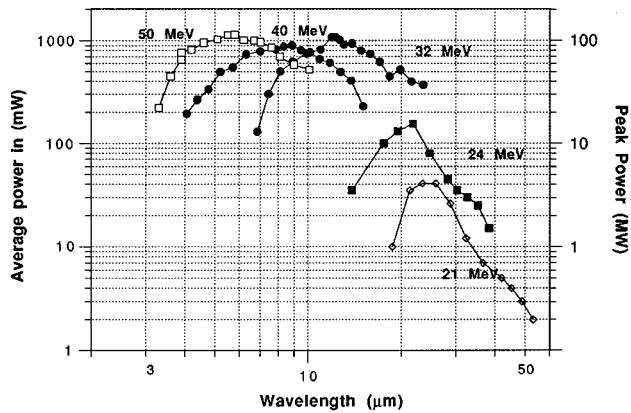


FIG. 3. CLIO spectral range. The average power is given at the repetition rate of 25 Hz (macropulses) and 62 MHz (micropulses). Higher rates can be used.

CSE scales linearly with the undulator length and quadratically with the current, whereas SASE scales exponentially.

### III. OBSERVATION OF CSE

The spontaneous emission enhancement is monitored through the signal delivered by an infrared detector (InSb or HgCdTe) placed on-axis in front of the undulator. The radiation is observed in an angular aperture sufficiently small to avoid spectral broadening when the spectrum is recorded. Production of either CSE or SASE requires different settings of the accelerator

(i) Quadrupoles settings in the bend: they act on the beam focusing in the undulator. Normally, they do not influence the CSE, which is sensitive only to the longitudinal shape of the bunch. However, this shape is sensitive to the magnetic elements acting on the bend isochronicity. Indeed, we found that CSE was less critically dependent on these tunings, since SASE is strongly influenced by the beam focusing in the undulator, as we will see below.

(ii) RF phases between the prebuncher, buncher, and accelerating section. These tunings act strongly on both the electron peak current and longitudinal shape, in a manner that cannot be predicted in practice: the CSE and SASE levels obtained being far from saturation, either one can be pro-

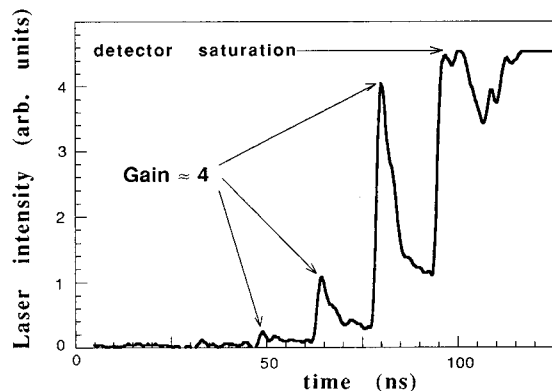


FIG. 4. CLIO optical gain measured at FEL start-up. The time delay between successive pulses is equal to the optical cavity roundtrip time.

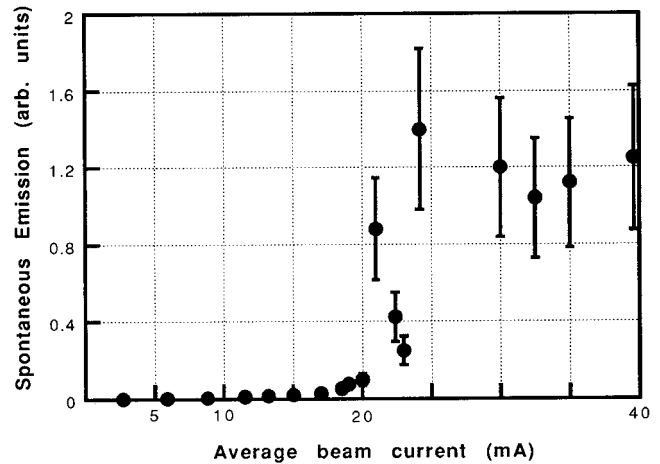


FIG. 5. Intensity dependence of CSE with the collimator slit position.

duced by a small substructure of the electron bunch such as a spike (CSE or SASE) or a sharp edge (CSE).

When one maximizes the spontaneous emission level to its maximum, one cannot predict whether the path taken will lead ultimately to CSE rather than SASE. Apparently, the optimization seems to favor only one type, rather than cause CSE and SASE to coexist. Therefore, they have to be distinguished by intensity and spectral measurements. Let us begin with CSE.

The intensity dependence of CSE has been measured, using the collimator placed in the bend (Fig. 5). The curve exhibits a step, far from the quadratic dependence expected for CSE. It can be understood, if we assume that the bunch has a substructure exhibited only by the particles possessing nearly the nominal energy (center of the curve). It is reasonable to think that the particles on the wings of the energy distribution have a smoother longitudinal distribution: they cannot contribute to CSE although they can still contribute to the electron peak current and, hence, to SASE, as we will see below.

The spectral behavior of the emitted radiation is the more convincing evidence: at any level of emission the spectral distribution is identical and possesses a constant spectral width of 3.3% (Fig. 6). The simple theory yields 2.3%, but the spectral width has always been found to be larger, due to inhomogeneous effects (emittance, in particular).

For clarity, the signals displayed in Fig. 6 are averaged: in fact, the noise affecting the CSE is of the order of 100%. This is due to the fact that very small changes in the bunch longitudinal shape produce very large changes in the high ranking Fourier coefficients: indeed, this would not happen at a wavelength longer than the electron bunch length. In our case, it is worthwhile to notice that we produce coherent emission at wavelengths (5–10  $\mu\text{m}$ ), of the order of  $10^{-3}$  of the electron bunch length. To our knowledge, this is the first time CSE is seen with such a small relative wavelength: previous studies [13,14] have also shown that CSE could be observed at wavelengths shorter than the electron bunch length, but only for a ratio greater than typically 5%.

### IV. OBSERVATION OF SASE

With the above parameters, the gain length  $L_g$  is about 1 m, and the saturation parameter is  $\rho(2N) = 0.07 \ll 1$  in our

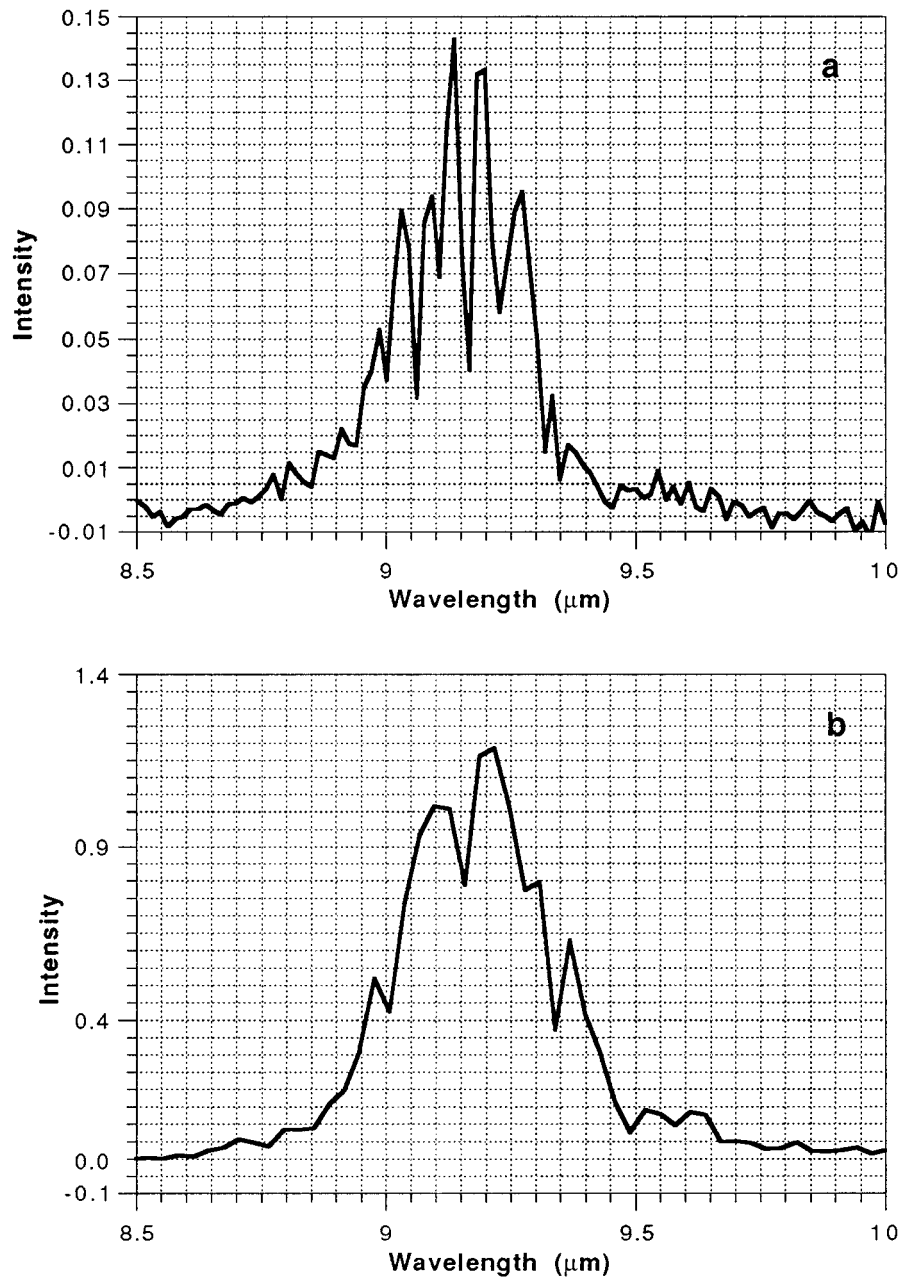


FIG. 6. Spectra of CSE at various levels: (a) minimum, (b) maximum.

case. This indicates that the SASE radiation is necessarily far from saturation, which would occur for 500 periods. For proper settings of the machine parameters, an appreciable level of SASE can be observed. It is very sensitive to the RF phase adjustments. The influence of such phase tuning, leaving the average current unchanged, is displayed in Fig. 7: the spontaneous emission intensity is strongly affected. One set of curves (“phase ON”) has been obtained with optimum RF phase adjustment, corresponding to a strong maximum of emission intensity, and the other set of curves (“phase OFF”) has been obtained with a detuned RF phase. While the average current remains constant, the peak current diminishes by approximately 50% [11]. This is evident proof that the SASE or CSE process occurs, since the SE is strictly proportional to the average current. The very strong observed effect calls for SASE rather than CSE. This is discussed below.

Figure 8 shows the spontaneous emission intensity as a function of the electron beam current with one or two undulators of an equal number of periods. Beam current has been varied by controlling the aperture of a beam slit of the collimator. Curve *A* (two undulators) exhibits clearly a nonlinear behavior (curve *B*, for one undulator, also, though less obvious) which implies a coherence effect such as CSE and/or SASE. The curve *C* is the curve *B* multiplied by a factor of 2. Since the CSE (and the SE) scales linearly with the undulator length, the difference between curves *A* and *C* is necessarily due to the presence of SASE. Therefore, SASE is present, which is also shown by its nonlinear behavior, although some CSE may also exist. It may occur also in the first undulator, which may be responsible for the small nonlinearity of curve *B*, but the accuracy is not sufficient to determine whether this behavior is exponential (SASE) or quadratic (CSE).

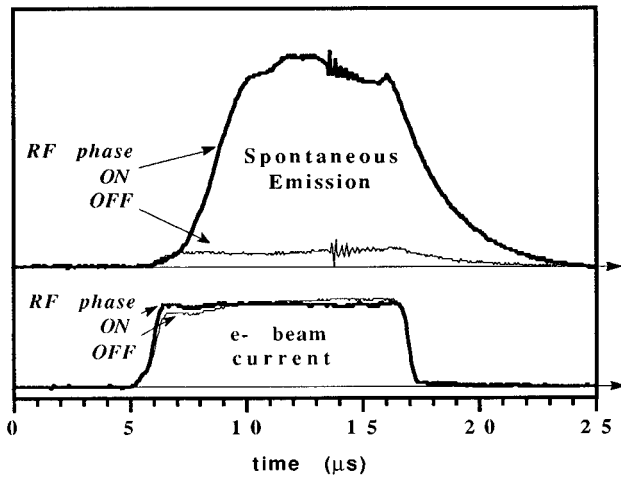


FIG. 7. Influence of the electron peak current (RF phase tuning) on the spontaneous intensity (top curves) during the electron macropulse. The bottom curves are the average electron beam currents.

These curves have been taken with an electron beam transverse size adjusted for the FEL oscillator. When one adjusts the size to maximize SASE, the intensity is only slightly increased by the presence of the second undulator: in this case the  $\rho$  parameter is maximized by a very small electron beam size in the center of the first undulator (Fig. 9). Then  $\rho$  becomes almost negligible in the second undulator, due to the divergence of the beam following a very small focus.

The spectrum of the SASE has been measured for various intensities of SASE. A spectrum is displayed in Fig. 10 for the case corresponding to the FEL beam adjustment of Fig. 9. It is taken at  $5 \mu\text{m}$ , so that we can use a sensitive InSb detector and measure both the SE and SASE: clearly a moderate amplification appears which is located at a slightly longer wavelength  $\Delta\lambda/\lambda = 1.4\%$ , close to the theoretical value of  $1/2N$  expected for FEL gain.

In Fig. 11, we display the spectra obtained with the best beam adjustment, at  $10 \mu\text{m}$ , where the detector (HgCdTe) is not sensitive enough to measure the SE: When SASE increases, the spectrum linewidth increases and the central wavelength shifts toward large values. The larger spectrum, corresponding to the higher SASE intensity, is displaced by

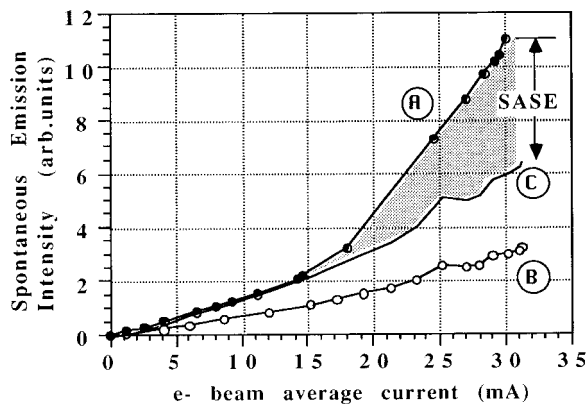


FIG. 8. Intensity of SASE vs electron beam current. Curves A and B correspond, respectively, to  $2N$  and  $N$  ( $= 19$ ) period undulators. Curve C is two times curve B.

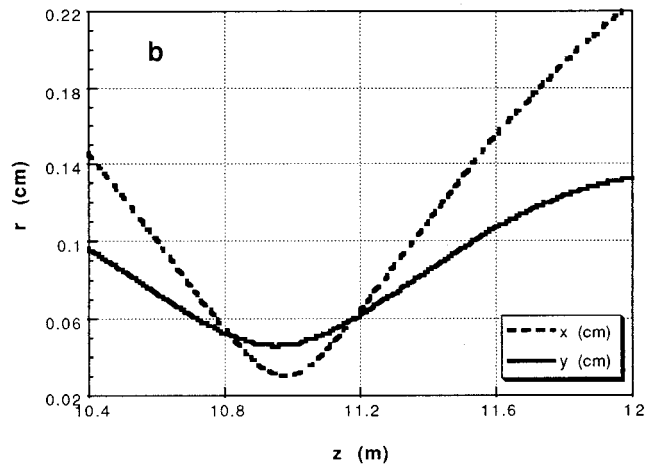
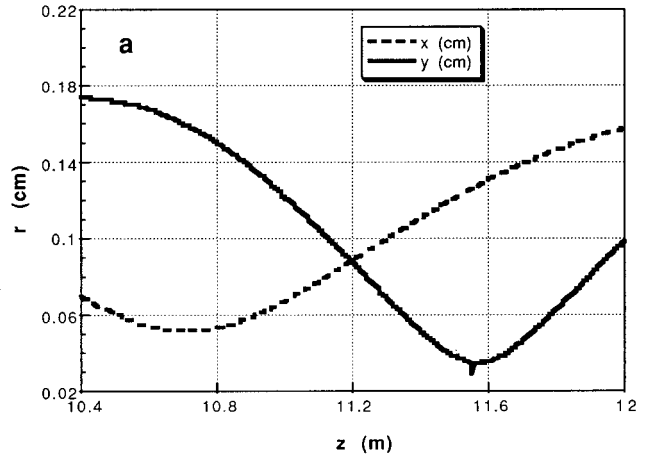


FIG. 9. Beam envelopes for FEL or CSE (a) and SASE experiments (b).

15% (at  $11.5 \mu\text{m}$ ), and has a linewidth of 23%. The resonance wavelength shift cannot be explained either by an angular error of 8 mrad or by a relative energy variation of 7%, which would cause large beam losses.

The experimental increase of the linewidth up to 23% is not in agreement with the SASE theory, which predicts a narrowing of the spectrum as compared to the SE. However,

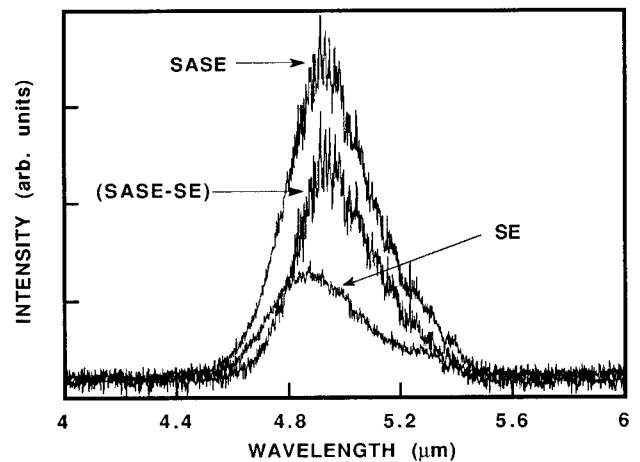


FIG. 10. Spectra of the emission with and without SASE and their difference at  $\lambda = 5 \mu\text{m}$ , with the "FEL" adjustment.

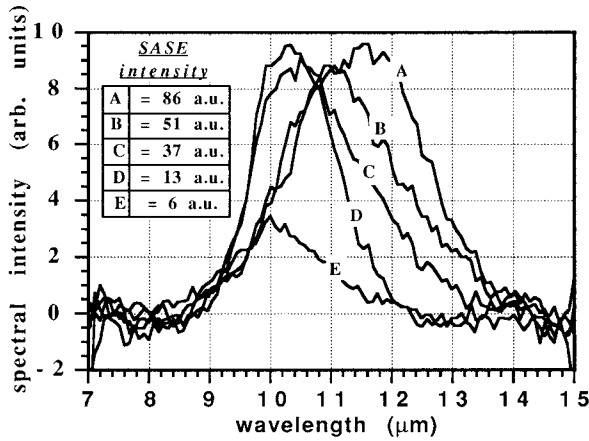


FIG. 11. Spectra of SASE for various SASE intensities (varying the linac peak current) for the best beam tuning at  $\lambda = 10 \mu\text{m}$ .

this theory considers the exponential growth of intensity rather than the start-up regime, as is the case here. Here, if we assume this width to be Fourier limited, a linewidth of  $\Delta\lambda/\lambda = 23\%$  corresponds to a wave train of about  $\Delta z \cong 40 \mu\text{m}$ . This value is 10 times shorter than the length,  $N\lambda = 400 \mu\text{m}$ , of the SE wave train. Such a short pulse regime is likely to be due to the fact that the electron bunch profile has a sharp maximum, which produces SASE, of the order of 1 ps, i.e.,  $300 \mu\text{m}$  or even shorter. This effective electron pulse length is of the order of the slippage length:  $200 \mu\text{m}$  for one undulator (since only one undulator appears to be efficient at the SASE best adjustment corresponding to Fig. 9). Therefore, the slippage reduces the overlap between the electrons and the wave train so that only a fraction of the SE wave train can be amplified, shortening the pulse and leading to the observed linewidth increase. The best phase tuning for SASE corresponds necessarily to the shortest spike in the electron bunch structure since the average current remains constant.

Finally, let us point out that CSE, like SASE, is very noisy. Figure 12 shows a SASE spectrum recorded without averaging: it consists in a series of lines. However, it is not clear whether this behavior comes from the expected spectral fluctuations of SASE or from its intensity fluctuations. The time dependence of SASE during the macropulse is shown in

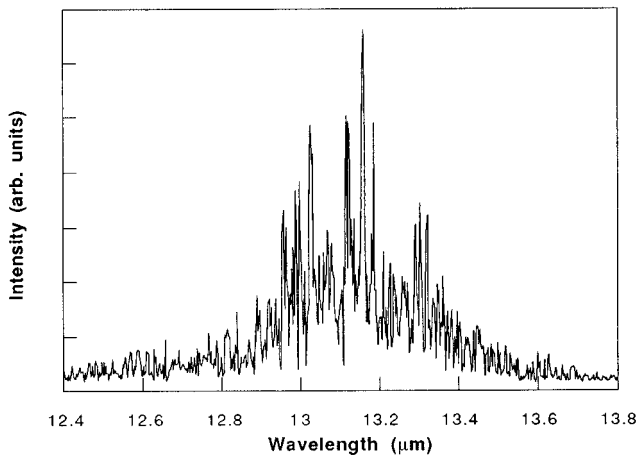


FIG. 12. SASE spectrum without averaging.

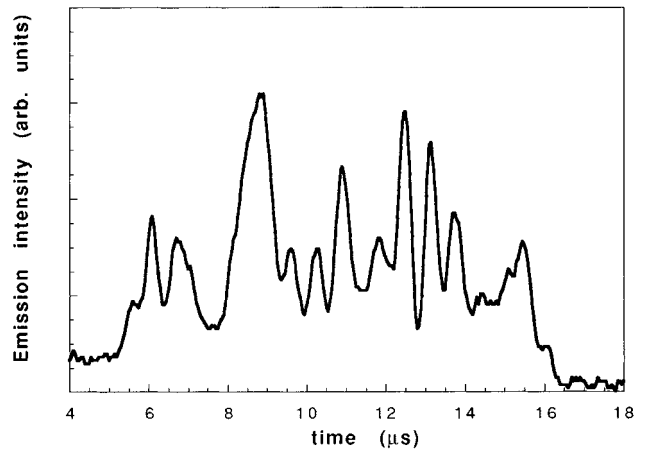


FIG. 13. SASE recorded with a time resolving detector.

Fig. 13, similar to Fig. 7 except it is recorded with a fast detector: it is extremely noisy along the macropulse. Besides the intrinsic unstable nature of below saturation SASE, this may be due to small RF phase variations (of the order of one degree [10]) which modify the bunch shape during the bunching process. Similar temporal behaviors have been recorded with CSE. Therefore a discrimination between CSE and SASE based on an analysis of the level of fluctuations is very difficult.

In conclusion, the good electron beam quality, which can be obtained with the CLIO machine, has allowed us to observe SASE in the midinfrared region, around 5 and  $10 \mu\text{m}$ . Although SASE is far from saturation, since the amplification is only one order of magnitude, we have been able to measure the spectral behavior at start-up and to observe an unexpected growth of the linewidth. In certain conditions, SASE is absent and CSE can be observed. Careful spectral measurements have allowed us to discriminate between them. The production of CSE at wavelength shorter than the electron bunch is a frequent situation: In the past, some attempts to produce a far-infrared FEL [15] or SASE [16] have resulted in emissions which seem dominated, rather, by CSE. In the present experiments, CSE happens at wavelengths as

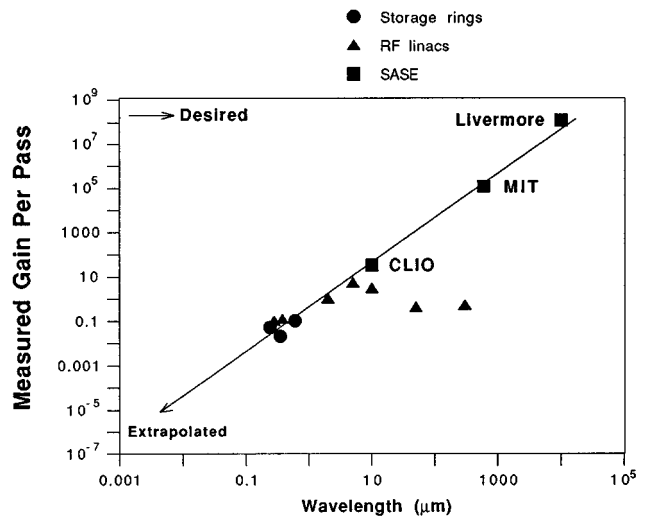


FIG. 14. Plot of the highest single pass amplifications presently obtained worldwide in free-electron devices.

short as  $10^{-3}$  of the electron bunch length. Therefore, CSE is likely to be observed as well in future experiments aimed at producing SASE at very short wavelengths [17,18], since these projects plan to use very short electron bunches. These will be produced, as in the case of CLIO, by velocity modulation imprinted in an accelerating element followed by a drift or a dispersive magnetic bend (magnetic compression). Since the electrons travel at nearly the speed of light, the deceleration is more efficient than the acceleration and the resulting pulse shape is always very nonsymmetric, with a sharp edge on one side producing short wavelength CSE.

In fact, SASE at short wavelength is very difficult to produce. A plot of the highest single pass amplifications obtained worldwide (Fig. 14) shows that approximately 15 orders of magnitude will have to be gained to generate SASE in the x-ray spectral region. Indeed, CSE could be an easier way to produce coherent light at short wavelength, since it is sensitive only to the longitudinal structure of the bunch but much less than SASE to its emittance and energy spread. Indeed, the number of photons generated by CSE would be smaller than would be produced by a fully saturated SASE process, but could be of some practical interest.

- 
- [1] Proceedings of the Free Electron Laser Conference: "FEL 1996," edited by G. Dattoli and A. Renieri, special issue of Nucl. Instrum. Methods Phys. Res. A **393** (1997).
- [2] *Laser Handbook*, edited by W. B. Colson, C. Pellegrini, and A. Renieri (North-Holland, Amsterdam, 1990), Vol. 6.
- [3] G. Kulipanov *et al.*, Nucl. Instrum. Methods Phys. Res. A **296**, 1 (1990).
- [4] R. Prazeres *et al.*, Europhys. Lett. **4**, 817 (1987).
- [5] F. Glotin *et al.*, Phys. Rev. Lett. **77**, 3130 (1996).
- [6] B. Bonifacio *et al.*, Opt. Commun. **50**, 373 (1984); J. Murphy and C. Pellegrini, Nucl. Instrum. Methods Phys. Res. A **237**, 159 (1985); K.-J. Kim, Phys. Rev. Lett. **57**, 1871 (1986).
- [7] T. Orzechowski *et al.*, Nucl. Instrum. Methods Phys. Res. A **250**, 144 (1986).
- [8] D. Kirkpatrick *et al.*, Nucl. Instrum. Methods Phys. Res. A **285**, 43 (1989).
- [9] R. Prazeres, J. M. Ortega, F. Glotin, D. A. Jaroszynski, and O. Marcouillé, Phys. Rev. Lett. **78**, 2124 (1997).
- [10] J. M. Ortega *et al.*, Nucl. Instrum. Methods Phys. Res. A **375**, 618 (1996); R. Chaput *et al.*, Nucl. Instrum. Methods Phys. Res. A **331**, 267 (1993).
- [11] F. Glotin *et al.*, Nucl. Instrum. Methods Phys. Res. A **341**, 49 (1994).
- [12] D. A. Jaroszynski *et al.*, Phys. Rev. Lett. **72**, 2387 (1994).
- [13] T. Nakazato *et al.*, Phys. Rev. Lett. **632**, 1245 (1989).
- [14] D. A. Jaroszynski *et al.*, Phys. Rev. Lett. **71**, 3798 (1993).
- [15] J. Lewellen *et al.*, Nucl. Instrum. Methods Phys. Res. A **358**, 24 (1995).
- [16] D. Bocek *et al.*, Nucl. Instrum. Methods Phys. Res. A **375**, 13 (1996); D. Bocek *et al.*, SLAC Report No. SLAC-PUB-7016 (1995).
- [17] J. Rossbach, Nucl. Instrum. Methods Phys. Res. A **375**, 269 (1996).
- [18] R. Tatchyn *et al.*, Nucl. Instrum. Methods Phys. Res. A **375**, 274 (1996).